

# FREQUENCY RESPONSE OF BLOOD FLOW AUTOREGULATION

NICHOLAS BRATTO\*, AFRAH HANEK, AND DAVID WENDL

FACULTY ADVISORS: DR. HYEJIN KIM AND DR. YULIA HRISTOVA

INDUSTRY MENTOR: DR. SEBASTIAN ACOSTA

**ABSTRACT.** Autoregulation is the capability of an organ such as the brain, heart, and kidney to maintain a constant blood flow over a series of changes in arterial pressure within their vascular beds. Since the organs in the human body demand a steady delivery of blood and bio-agents to sustain their metabolic activity, autoregulation is crucial in protecting the organs from both over and under perfusion of blood. The impairment of autoregulation may lead to neurological, renal, and other complications. In this study, we analyze a simplified and recently developed mathematical model of blood flow autoregulation based on a system of nonlinear ordinary differential equations. Utilizing this model, we develop the optimal and realistic wall-compliance profiles of the blood vessels. Using the realistic wall-compliance profile, we then find the frequency response of the autoregulation system. The frequency response can be used to determine whether an organ is autoregulating or not given some input frequency.

## 1. INTRODUCTION

Autoregulation is an extremely important mechanism that keeps blood flow and volume stable in the circulatory system. The circulatory system regulates the blood flow and supply of nutrients, vitamins, minerals, oxygen, carbon dioxide, hormones, metabolic waste and more to meet functional needs of tissues, muscles, and organs. The basic components of the system consists of the heart, arteries, capillary beds, and veins. The heart pumps the blood, the arteries carry oxygenated blood away from the heart into the capillary beds, the capillary beds carry deoxygenated blood to the veins, and the veins carry the deoxygenated blood back to the heart. Organ vasculature attempts to diminish changes in blood flow induced by changes in arterial pressure. This control, known as autoregulation, is accomplished by adapting vascular stiffness which fluctuates by dilation or constriction. There are many contributing factors and accompanying studies as to what controls the autoregulation mechanism and response especially regarding the myogenic response—how arterioles physically adjust by expanding and contracting and the tubuloglomerular feedback response—“localized” information of ion content of the fluid in the kidneys being sensed and the arterioles adjusting accordingly [2]. This study will focus on the hemodynamic parameters associated with the myogenic response of autoregulation.

Most organs exhibit a certain degree of blood flow autoregulation. If blood pressure through an organ’s arteries becomes too low or too high, the system fails to maintain a constant blood flow. The brain needs to autoregulate the most because brain cells cannot tolerate an under or over supply of blood without getting damaged [2]. A normal functioning autoregulatory mechanism within certain pressure limits could be the difference between life and death for a small child with a severe concussion, for example. Physicians can monitor a “relative” blood volume using NIRS sensors (near-infrared spectroscopy) or by measuring intracranial pressure which moves in phase with blood volume [3].

Autoregulation has been studied and analyzed in both human and animal bodies using several different types of mathematical models based on Navier–Stokes equations, stochastic differential equations, ordinary differential equations, and Windkessel models (for examples, see [1], [5], and [8]). In this study, we analyze a

---

*Key words and phrases.* Autoregulation, frequency response, hemodynamics, mathematical model, nonlinear differential equations, wall-compliance.

This research project was conducted during the MAA 2016 PIC Math at the University of Michigan–Dearborn and it was provided by Dr. Sebastian Acosta from Texas Children’s Hospital. PIC Math program was sponsored by the National Science Foundation (NSF grant DMS-1345499).

\* Corresponding author.

mathematical model based on a system of nonlinear ordinary differential equations. The model is a simplified version of a stochastic hemodynamic model with the autoregulation mechanism [1]. Though the model is simpler and not as sophisticated as models based on Navier–Stokes equations or stochastic differential equations, the analysis performed still provides enough accurate and valuable information.

The motivation of this study is to help doctors determine if autoregulation is taking place in a patient by utilizing this mathematical model of blood flow autoregulation. The ultimate goal of the autoregulatory mechanism is to keep blood flow constant to all organs and tissues. However, measuring a patient’s blood flow is very difficult and time consuming in a realistic medical setting. So, how can a doctor tell if a patient’s blood flow is autoregulating or not?

The remainder of this paper is organized as follows: Section 2 introduces and analyzes the mathematical model to describe the flow of blood through an organ. In Subsection 2.1, we study and utilize the optimal and realistic autoregulation models to come up with a complete autoregulatory wall–compliance profile. Next, in Subsection 2.2, we develop and find the frequency response of the autoregulation system by using the autoregulatory wall–compliance profile we find in Subsection 2.1 and solve for the optimal frequency for a regulating response. Finally, in Section 3, we draw our conclusions and discuss the results.

## 2. MODEL

**2.1. Wall–Compliance and Optimal Autoregulation.** A new mathematical model describing the flow of blood through an organ has been recently developed by Acosta et al. [1]. The model consists of a system of two nonlinear ordinary differential equations for the blood pressure through an organ  $P$ , the flow rate through an organ  $Q$ , and an algebraic equation relating the pressure through an organ  $P$  to the volume of blood  $V$  contained in the organ. The system is the following:

$$(1) \quad L_{\text{ref}} \left[ \frac{V_{\text{ref}}}{V} \right] \frac{dQ}{dt} + R_{\text{ref}} \left[ \frac{V_{\text{ref}}}{V} \right]^2 Q = P_a - P,$$

$$(2) \quad \frac{dV}{dt} = Q - Q_v,$$

$$(3) \quad V = V_{\text{ref}} (1 + \Gamma P)^2.$$

Here  $R_{\text{ref}}$ ,  $L_{\text{ref}}$  and  $V_{\text{ref}}$  represent reference values which are constants for resistance, inertance and blood volume. The arterial pressure is denoted by  $P_a$ , the flow rate into the veins is denoted by  $Q_v$ , and the symbol  $\Gamma$  denotes the wall–compliance (inverse of stiffness) of the blood vessels. Note that the wall–compliance is not a constant but a function of blood pressure which models the autoregulatory mechanism. Autoregulation will allow a change in the volume of blood in the organ, which induces changes in the resistance, which induces changes in the blood flow to counter the variations in arterial pressure. The autoregulation mechanism functions to control the flow rate, not to control the pressure. The following profile has been suggested as a realistic model:

$$(4) \quad \Gamma = \gamma \exp \left\{ -\frac{P}{\pi_o} \right\},$$

where  $\gamma$  is the baseline value for the vascular wall–compliance of an organ and  $\pi_o$  represents how sensitive the vascular wall–compliance is to changes in pressure. Both  $\gamma$  and  $\pi_o$  are constants to be determined in this section for the wall–compliance  $\Gamma$ . Additionally, we will be using reference parameters provided by Dr. Acosta from Texas Children’s Hospital listed below:

Name	Symbol	Value	Units
Reference volume	$V_{\text{ref}}$	20	$\text{cm}^3$
Reference inertance	$L_{\text{ref}}$	1.0	$\text{g}/\text{cm}^4$
Reference resistance	$R_{\text{ref}}$	5.0	$\text{mmHg}/\text{cm}^3$
Venous flow rate	$Q_v$	10	$\text{cm}^3/\text{s}$
Baseline flow rate	$Q_{\text{base}}$	10	$\text{cm}^3/\text{s}$

The first objective is to find and study the optimal wall-compliance profile  $\Gamma_{\text{opt}}$  by using the realistic model of autoregulation  $\Gamma = \gamma \exp\{- (P/\pi_o)\}$  and manipulating our system of equations (1)–(3). We will find  $\Gamma_{\text{opt}}$  as a function of the pressures  $P_a$  and  $P$  under the constraint  $Q = Q_{\text{base}}$ , where  $Q_{\text{base}}$  is the baseline flow rate demanded by the organ. We will assume that  $P_a = P/\theta$  where  $\theta \in (0, 1)$ . The second objective will be to find the constants  $\gamma$  and  $\pi_o$ . This will allow us to develop the frequency response of the system in Subsection 2.2.

Let us find a profile for  $\Gamma$  such that under quasi-steady conditions  $dQ/dt = 0$  so that we can guarantee that  $Q = Q_{\text{base}}$ . Implementing these two conditions will yield the optimal profile  $\Gamma_{\text{opt}}$ . This will be an optimal profile because it optimizes the purpose of autoregulation which is to keep the flow of blood constant through an organ while using the baseline flow rate. Using (1) and (3):

$$L_{\text{ref}} \left[ \frac{V_{\text{ref}}}{V} \right] \frac{dQ}{dt} + R_{\text{ref}} \left[ \frac{V_{\text{ref}}}{V} \right]^2 Q = P_a - P$$

becomes

$$R_{\text{ref}} Q_{\text{base}} \left[ (1 + \Gamma P)^{-2} \right]^2 = (P_a - P).$$

Solving for the function  $\Gamma$  which will be denoted by  $\Gamma_{\text{opt}}$ , we obtain an optimal wall-compliance profile  $\Gamma_{\text{opt}}(P)$ :

$$\Gamma_{\text{opt}}(P) = \frac{1}{P} \left[ \left[ \frac{R_{\text{ref}} Q_{\text{base}}}{P_a - P} \right]^{\frac{1}{4}} - 1 \right].$$

Using the fact that  $P_a = P/\theta$  for  $0 < \theta < 1$ , we have

$$(5) \quad \Gamma_{\text{opt}}(P) = \frac{1}{P} \left[ \left[ \frac{R_{\text{ref}} Q_{\text{base}}}{\left(\frac{1}{\theta} - 1\right)P} \right]^{\frac{1}{4}} - 1 \right].$$

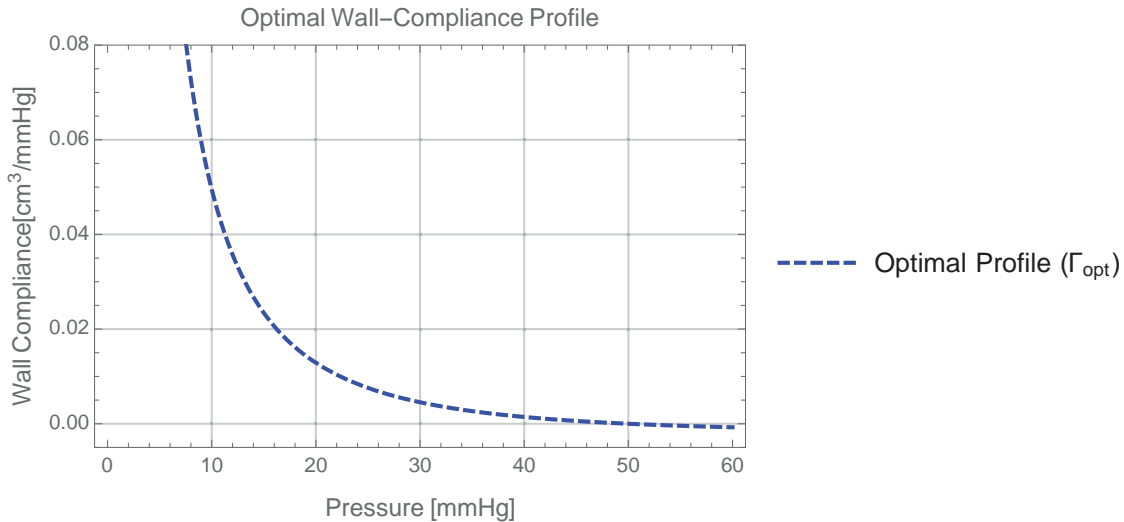


FIGURE 1. Plot of (5). Here  $R_{\text{ref}} = 5.0 \text{ mmHg}/\text{cm}^3$ ,  $Q_{\text{base}} = 10 \text{ cm}^3/\text{s}$  and  $\theta = 0.5$ . As instructed by Dr. Acosta, we choose  $\theta = 0.5$  for simplicity, so that the denominator in (5) is equal to  $P$ . As blood pressure increases, the wall-compliance of the blood vessels is decreasing. Also, note that  $\Gamma$  in general must be positive to make physical sense.

In Figure 1, we can observe that the blood vessels are getting stiffer as pressure increases. Mathematically, the optimal profile  $\Gamma_{opt}$  behaves similar to the realistic model of wall-compliance  $\Gamma$  in that both functions decay exponentially. Using this correlation will help us to determine the unknown parameters  $\gamma$  and  $\pi_o$  so that (4) provides good autoregulation. To find both constants  $\gamma$  and  $\pi_o$  for the realistic model  $\Gamma = \gamma \exp\{- (P/\pi_o)\}$ , we will compare the two profiles of  $\Gamma_{opt}$  and  $\Gamma$  in Figure 2 to find where the profile  $\Gamma$  is tangent and equal to the optimal profile  $\Gamma_{opt}$ . It is at the reference pressure of  $P_{ref} = P = 25$  mmHg, which represents the average pressure of a new born baby provided by Dr. Acosta, that  $\Gamma$  is tangent and exactly equal to the optimal profile  $\Gamma_{opt}$ .

First, we will solve for  $\pi_o$  by using the slope of  $\Gamma'(P)$  and  $\Gamma'_{opt}(P)$ . Setting  $\Gamma'(P)$  equal to  $\Gamma'_{opt}(P)$  at  $P = 25$  mmHg:

$$\begin{aligned} \Gamma'(P) &= \Gamma'_{opt}(P) \\ (6) \quad -\frac{\gamma}{\pi_o} \exp\left\{-\frac{P}{\pi_o}\right\} &= \frac{1}{P^2} \left[ 1 - \frac{5}{4} \left( \frac{R_{ref} Q_{base}}{(\frac{1}{\theta} - 1)P} \right)^{1/4} \right]. \end{aligned}$$

Due to  $\Gamma(P) = \Gamma_{opt}(P)$  at  $P = 25$  mmHg, the left hand side of (6) can be rewritten as follows:

$$-\frac{1}{\pi_o} \gamma \exp\left\{-\frac{P}{\pi_o}\right\} = -\frac{1}{\pi_o} \Gamma(P) = -\frac{1}{\pi_o} \Gamma_{opt}(P), \quad \text{if } P = 25 \text{ mmHg.}$$

Therefore (6) becomes

$$\frac{1}{\pi_o} \left\{ \frac{1}{P} \left( 1 - \left[ \frac{R_{ref} Q_{base}}{(\frac{1}{\theta} - 1)P} \right]^{1/4} \right) \right\} = \frac{1}{P^2} \left[ 1 - \frac{5}{4} \left( \frac{R_{ref} Q_{base}}{(\frac{1}{\theta} - 1)P} \right)^{1/4} \right].$$

Solving for  $\pi_o$  we have

$$\pi_o = P \frac{\left( 1 - \left[ \frac{R_{ref} Q_{base}}{(\frac{1}{\theta} - 1)P} \right]^{1/4} \right)}{\left( 1 - \frac{5}{4} \left[ \frac{R_{ref} Q_{base}}{(\frac{1}{\theta} - 1)P} \right]^{1/4} \right)}, \quad \text{for } 0 < \theta < 1.$$

Using  $\theta = 0.5$  and  $P = 25$  mmHg, we obtain

$$\pi_o \simeq 9.7226955.$$

Next, to solve for  $\gamma$  we will use  $\Gamma(P)$  and  $\Gamma_{opt}(P)$ . Setting  $\Gamma(P)$  equal to  $\Gamma_{opt}(P)$ :

$$\begin{aligned} \Gamma(P) &= \Gamma_{opt}(P) \\ (7) \quad \gamma \exp\left\{-\frac{P}{\pi_o}\right\} &= \frac{1}{P} \left[ \left[ \frac{R_{ref} Q_{base}}{(\frac{1}{\theta} - 1)P} \right]^{1/4} - 1 \right]. \end{aligned}$$

Solving for  $\gamma$  we have

$$\gamma = \exp\left\{-\frac{P}{\pi_o}\right\} \frac{1}{P} \left[ \left[ \frac{R_{ref} Q_{base}}{(\frac{1}{\theta} - 1)P} \right]^{1/4} - 1 \right].$$

Thus, by using the fact that  $\pi_o = 9.7226955$ ,  $P = 25$  mmHg, and choosing  $\theta = 0.5$ , we obtain

$$\gamma \simeq 0.0990148.$$

Therefore, the realistic wall-compliance  $\Gamma$  is given by

$$\Gamma(P) = 0.0990148 \times \exp \left\{ -\frac{P}{9.7226955} \right\},$$

whose graph is plotted in Figure 2 with the optimal profile  $\Gamma_{\text{opt}}$ . Note that in Figure 2, the realistic profile is only a close approximation to the optimal profile near  $P = 25$  mmHg. Further away from this point for increases in pressure, the realistic and optimal profiles start to behave differently. Notice that as the pressure increases toward infinity, the realistic profile tends toward zero and the optimal profile becomes negative, which does not make physical sense.

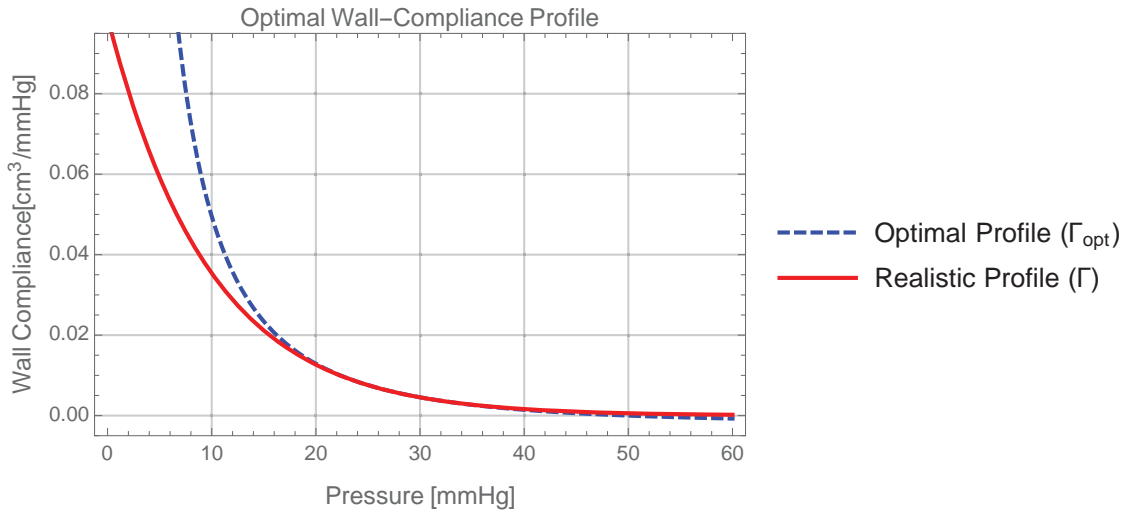


FIGURE 2. [Color online] Plot of the optimal and realistic wall-compliance profiles. Here  $R_{\text{ref}} = 5.0$  mmHg/cm<sup>3</sup>,  $Q_{\text{base}} = 10$  cm<sup>3</sup>/s and  $\theta = 0.5$ . Using our values for  $\gamma \simeq 0.0990148$  and  $\pi_o \simeq 9.7226955$ , our realistic profile is plotted side-by-side with our optimal profile. The two profiles are similar especially in the range of about 22–35 mmHg where they are intersecting.

Now that we have a realistic profile for wall-compliance,  $\Gamma$  from (4), we want to see how well (1) regulates blood flow at different pressures using the realistic profile for wall-compliance. To test this, we will manipulate (1) and (3) in such a way as to finding blood flow  $Q$  as a function of pressure  $P$ . Also, since we would like to find a steady solution, we will assume that  $dQ/dt = 0$ . Under this assumption, the equation for blood flow is

$$Q = \frac{1}{R_{\text{ref}}} \left( \left( \frac{1}{\theta} - 1 \right) P \right) \left( 1 + \gamma P \exp \left\{ -\frac{P}{\pi_o} \right\} \right)^4.$$

In Figure 3, we see that our realistic wall-compliance profile regulates blood flow well within a range around 22 mmHg to 35 mmHg. This is due to our realistic wall-compliance profile deviating from our optimal profile, as explained above.

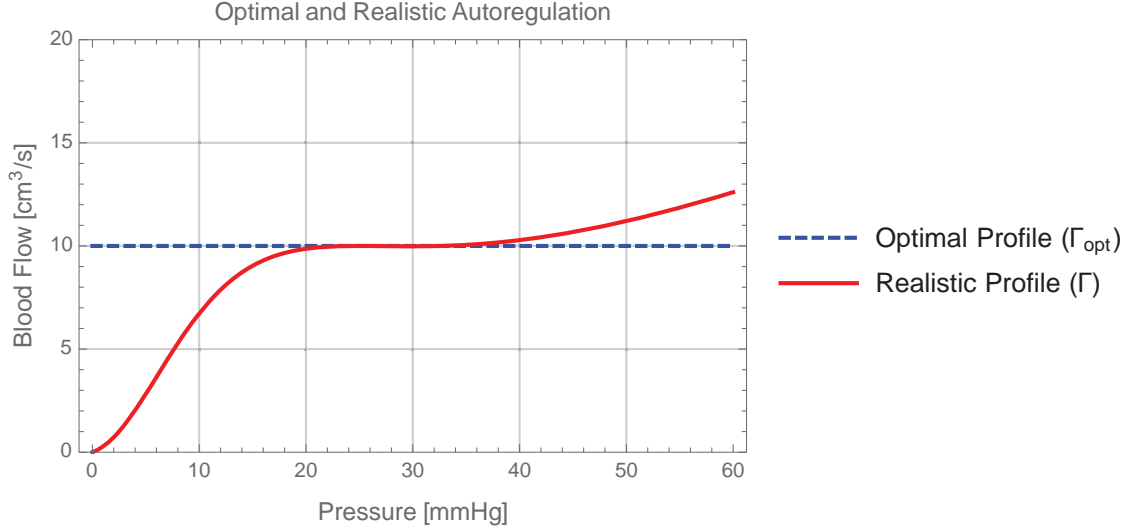


FIGURE 3. [Color online] The graph for blood flow  $Q$  under the assumption of  $dQ/dt = 0$  and using  $\Gamma_{\text{opt}}(P)$  and  $\Gamma$ . The realistic profile shows that blood flow is maintained reasonably constant from about 22–35 mmHg, signifying that the autoregulation mechanism is actively adjusting quite well to changes in pressure.

**2.2. Frequency Response.** The second objective of this study is to find the frequency response of the autoregulation system and the optimal frequency for a regulating response by using (1)–(3) and the autoregulatory profile (4) with the constants  $\gamma$  and  $\pi_o$  that were found in Subsection 2.1. We are especially interested in two relationships: the amplitude gain from arterial pressure oscillations to flow rate oscillations and the phase shift from arterial blood pressure to blood volume. This will provide useful information regarding the detection and time delay of autoregulation response for some input frequency.

We assume that the arterial pressure  $P_a$  oscillates harmonically about a fixed reference value:  $P_a = P_{a,\text{ref}}(1 + \epsilon e^{i\omega t})$  with small  $\epsilon$ . First, we will define the *global wall-compliance* for the entire organ vascular bed by using (3):

$$(8) \quad C = \frac{dV}{dP} = 2V_{\text{ref}}\bar{\Gamma}(1 + \bar{\Gamma}P),$$

where the “overline” represents a time averaged value. Here we define

$$C_{\text{ref}} = 2V_{\text{ref}}\Gamma_{\text{ref}}(1 + \Gamma_{\text{ref}}P_{\text{ref}}),$$

where  $\Gamma_{\text{ref}} = \gamma \exp\{- (P_{\text{ref}}/\pi_o)\}$  with  $P_{\text{ref}} = 25$  mmHg. By using (2) we have

$$(9) \quad \frac{dV}{dt} = \frac{dV}{dP} \frac{dP}{dt} = C \frac{dP}{dt} = Q - Q_v.$$

Assuming that the venous outflow rate  $Q_v$  is constant we obtain

$$(10) \quad C \frac{d^2P}{dt^2} = \frac{dQ}{dt}.$$

Now, we combine (9), (10), and (1) to obtain a second order differential equation for the pressure:

$$(11) \quad LC \frac{d^2 P}{dt^2} + RC \frac{dP}{dt} + P = \bar{P}_a (1 + \epsilon e^{i\omega t}) - RQ_v.$$

Here,  $L = L_{\text{ref}}$ ,  $R = R_{\text{ref}}$ , and  $C = C_{\text{ref}}$ . For the remainder of the paper, we will use  $L$ ,  $R$ , and  $C$  to denote each reference value for convenience of notation.

We will solve (11) analytically to understand the behavior of pressure with respect to time. We will find both the homogeneous and inhomogeneous solutions to (11). Observing the right hand side of (11), the inhomogeneous solution will need to consist of two terms: a steady term which depends on  $P_a$  and  $RQ_v$  and another term that oscillates with a frequency  $\omega$ .

First, we find the homogeneous solution of (11):

$$(12) \quad \frac{d^2 P}{dt^2} + \frac{R}{L} \frac{dP}{dt} + \frac{1}{LC} P = 0.$$

By setting  $P(t) = \exp\{rt\}$  with a constant variable  $r$ , (12) becomes

$$\left( r^2 + \frac{R}{L} r + \frac{1}{LC} \right) P(t) = 0.$$

Thus, the constant  $r$  must be

$$(13) \quad r = \frac{1}{2} \frac{R}{L} \left( -1 \pm \sqrt{1 - \frac{4L}{CR^2}} \right).$$

By substituting all reference values back into (13), the homogeneous solution of (11) is

$$P_{\text{homo}}(t) = C_1 \exp\{r_1 t\} + C_2 \exp\{r_2 t\},$$

where  $C_1$  and  $C_2$  are unknown constants and  $r_1 = -4.3634135$  and  $r_2 = -0.636586$ . We are only concerned with the long-term behavior of our solutions. Since both  $r_1$  and  $r_2$  are negative, the homogenous solution will quickly decay exponentially. Thus, we can safely neglect the homogeneous solution  $P_{\text{homo}}(t)$  for the long-term behavior of our solutions.

Next, we need to find the inhomogeneous solution of (11). Let the inhomogeneous solution be

$$P_{\text{inhomo}}(t) = \alpha + (\beta + \kappa i) \exp\{i\omega t\}.$$

By substituting the inhomogeneous solution back into (11) and solving for  $\alpha$ ,  $\beta$  and  $\kappa$ , we have

$$\begin{aligned} \alpha &= \bar{P}_a - RQ_v, \\ \beta &= \frac{\epsilon \bar{P}_a (1 - LC\omega^2)}{(1 - LC\omega^2 + (CR)^2 \omega^2)}, \\ \kappa &= \frac{-\epsilon \bar{P}_a (-\omega RC)}{(1 - LC\omega^2 + (CR)^2 \omega^2)}. \end{aligned}$$

Substituting  $\alpha$ ,  $\beta$  and  $\kappa$  back into the inhomogeneous solution  $P_{\text{inhomo}}(t)$  and simplifying, we obtain the inhomogeneous solution:

$$(14) \quad P_{\text{inhomo}}(t) = \bar{P} + \frac{\epsilon \bar{P}_a \exp\{i\omega t\}}{1 + iRC\omega - LC\omega^2}.$$

Here, the amplitude gain from the arterial pressure oscillations to flow rate oscillations is given by

$$(15) \quad \text{amplitude} = |\beta + \kappa i| = \sqrt{\beta^2 + \kappa^2} = \frac{\epsilon \bar{P}_a}{\sqrt{(1 - LC\omega^2 + (CR)^2\omega^2)}}.$$

Now, we will test  $P_{\text{inhomo}}(t)$  with different frequencies  $\omega$ , in Hz, and plot this function  $P_{\text{inhomo}}(t)$  in Figure 4. We can observe from Figure 4 as the frequency increases, the amplitude of the pressure oscillations decreases. The amplitude gain is influenced significantly by the frequency and in addition influences the time delay between pressure oscillations. A lower frequency will result in longer time delays while a higher frequency will result in shorter time delays. The lower the frequency is, the easier it is to tell if an organ is autoregulating or not [3].

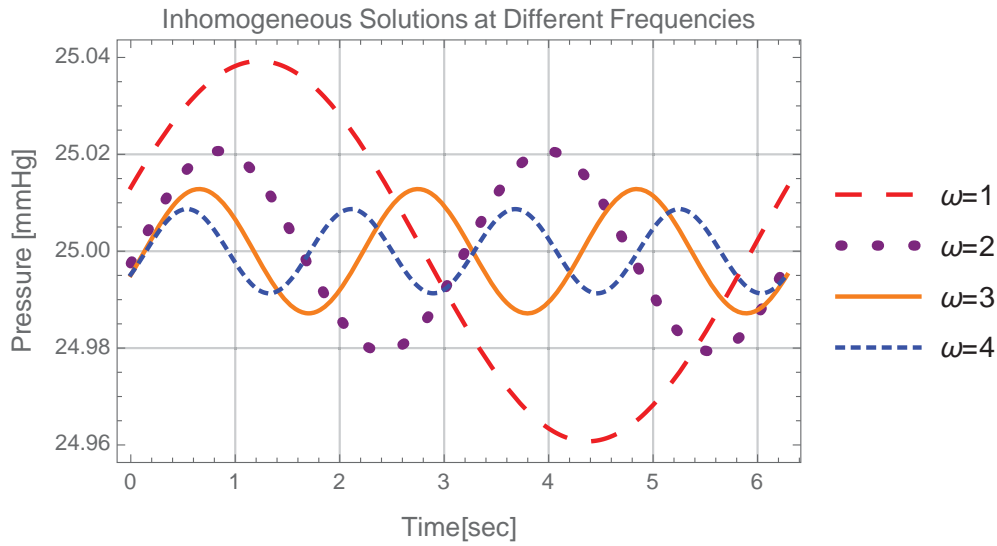


FIGURE 4. [Color online] Plot of the inhomogeneous solutions with incrementally increasing frequencies. We observe that as the frequencies increase, the amplitude of the arterial pressure oscillations decrease as well as the period—the time it takes to complete a cycle.

Hereafter, for convenience of notation, we will use  $P(t)$  to denote  $P_{\text{inhomo}}(t)$  from (14) in order to study the long term behavior of pressure by neglecting the homogeneous solution. We will first plug  $P(t)$  into the wall-compliance  $\Gamma(P) = \gamma \exp\{- (P/\pi_o)\}$  and then expand the expressions in the wall-compliance  $\Gamma$  in powers of  $\epsilon$ :

$$\Gamma(P) = \gamma \exp \left\{ -\frac{1}{\pi_o} \left( \bar{P} + \frac{\epsilon \bar{P}_a \exp\{i\omega t\}}{1 + iRC\omega - LC\omega^2} \right) \right\},$$

which can be rewritten as

$$\begin{aligned} \Gamma(P) &= \gamma \exp \left\{ -\frac{\bar{P}}{\pi_o} \right\} \times \exp \left\{ -\frac{1}{\pi_o} \frac{\epsilon \bar{P}_a \exp\{i\omega t\}}{(1 + iRC\omega - LC\omega^2)} \right\} \\ &= \bar{\Gamma} \times \exp \left\{ -\frac{1}{\pi_o} \frac{\epsilon \bar{P}_a \exp\{i\omega t\}}{(1 + iRC\omega - LC\omega^2)} \right\}. \end{aligned}$$

From the linearization or expanding the expressions in the wall-compliance  $\Gamma$  in powers of  $\epsilon$ , the wall-compliance  $\Gamma$  is given by

$$(16) \quad \Gamma(P) = \bar{\Gamma} \times \left( 1 - \frac{1}{\pi_o} \left( \frac{\epsilon \bar{P}_a \exp \{i\omega t\}}{(1 + iRC\omega - LC\omega^2)} \right) + \mathcal{O}(\epsilon^2) \right),$$

where  $\bar{\Gamma} = \gamma \exp \{ -(\bar{P}/\pi_o) \}$ .

Next, we plug (14) and (16) into (3) and expand (3) yielding

$$V = V_{\text{ref}} \left[ 1 + \left( \bar{\Gamma} \left( 1 - \frac{1}{\pi_o} \left( \frac{\epsilon \bar{P}_a \exp \{i\omega t\}}{(1 + iRC\omega - LC\omega^2)} \right) + \mathcal{O}(\epsilon^2) \right) \right) \left( \bar{P} + \frac{\epsilon \bar{P}_a \exp \{i\omega t\}}{1 + iRC\omega - LC\omega^2} \right) \right]^2,$$

which can be simplified to

$$V = V_{\text{ref}} (1 + \bar{\Gamma} \bar{P})^2 + (2V_{\text{ref}}(1 + \bar{\Gamma} \bar{P}) \bar{\Gamma} (1 - \bar{P}/\pi_o)) \left( \frac{\epsilon \bar{P}_a \exp \{i\omega t\}}{1 + iRC\omega - LC\omega^2} \right).$$

We neglect  $\mathcal{O}(\epsilon^2)$  series terms because they are numerically insignificant contributions, due to epsilon being very small. To show this, we will formulate and plot two active autoregulating equations: one with the  $\mathcal{O}(\epsilon^2)$  series terms and one truncated without the  $\mathcal{O}(\epsilon^2)$  series terms.

For *active* autoregulation we obtain

$$(17) \quad V = \bar{V} + C_{\text{auto}} \frac{\epsilon \bar{P}_a \exp \{i\omega t\}}{1 + iRC\omega - LC\omega^2} + \mathcal{O}(\epsilon^2)$$

and for *active, truncated* autoregulation we have

$$(18) \quad V = \bar{V} + C_{\text{auto}} \frac{\epsilon \bar{P}_a \exp \{i\omega t\}}{1 + iRC\omega - LC\omega^2},$$

where  $\bar{V} = V_{\text{ref}}(1 + \bar{\Gamma} \bar{P})^2$  and  $C_{\text{auto}} = 2V_{\text{ref}}(1 + \bar{\Gamma} \bar{P}) \bar{\Gamma} (1 - \bar{P}/\pi_o)$ . We define the variables  $\bar{V}$  and  $C_{\text{auto}}$  here as being in the active autoregulation state because the wall-compliance  $\bar{\Gamma}$  is a function of pressure  $\bar{P}$ . When  $\bar{\Gamma}$  is not a function of  $\bar{P}$  then  $\bar{\Gamma} = \gamma$  in (18), representing that the wall-compliance is constant and autoregulation is *inactive*.

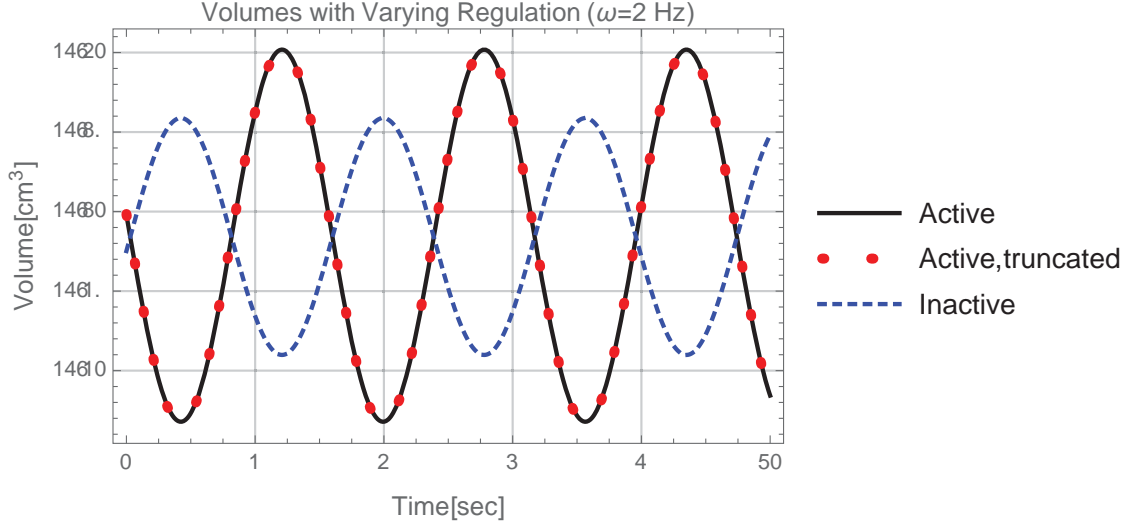


FIGURE 5. [Color online] Plot of volumes with varying regulation profiles from (17) and (18). The inactive profile is  $180^\circ$  out-of-phase with both active profiles. As the phase shift decreases from  $180^\circ$  to  $0^\circ$ , the active profiles will “shift” toward the inactive profile, which would make it increasingly difficult to determine if autoregulation is occurring or not.

First, we can observe that the regulating volume (17) and the truncated regulating volume (18) profiles perfectly overlap in Figure 5. This serves as further justification for omitting the  $\mathcal{O}(\epsilon^2)$  terms. The inactive regulating volume profile is plotted when the wall-compliance  $\bar{\Gamma}$  is constant, it is not a function of pressure in (18). This indicates that the wall-compliance function is not adjusting to pressure fluctuations.

Secondly, we can observe that the inactive regulating volume profile in Figure 5 is always  $180^\circ$  out-of-phase with the regulating volume profiles for any frequency  $\omega$ . Mathematically, we can calculate that  $C_{\text{auto}}$  will always be negative given any pressure  $\bar{P}$ . Both observations are important results in that one can confirm mathematically if an organ’s arteries, vascular bed, or area of the circulatory system is actively autoregulating at some input frequency. Good autoregulation is therefore reflected as volume moves out of phase with respect to pressure. In contrast, poor autoregulation is reflected when volume moves in phase with pressure, signifying from the mathematical model that the vasculature is not reacting at all or  $\bar{\Gamma}=\text{constant}$ . Therefore, a physical connection can be made that if the wall-compliance of the blood vessels is not changing with fluctuating pressure, then the autoregulatory mechanism is not working properly.

Lastly, we are interested in the phase shift between the arterial pressure and volume as a function of the frequency  $\omega > 0$ . From (17), the frequency response or the transfer function  $T_{P_a \rightarrow V}$  (for more information on transfer functions refer to [7]) from the arterial pressure oscillations to volume oscillations is given by

$$(19) \quad T_{P_a \rightarrow V}(\omega) = \frac{C_{\text{auto}}}{1 + iRC\omega - LC\omega^2}.$$

This transfer function will indicate how out-of-phase an active regulating response would be to an inactive regulating response. By taking the argument of our complex number, we will be able to determine this phase shift  $\theta$  and must solve for optimal frequency. To see what phase shift  $\theta$  would result in a frequency  $\omega$ , set

$$\theta = \arg\left(\frac{1}{1 + iRC\omega - LC\omega^2}\right) = \tan^{-1}\left(\frac{RC\omega}{LC\omega^2 - 1}\right).$$

We then have

$$(20) \quad LC\omega^2 - RC\omega \cot(\theta) - 1 = 0.$$

We choose  $\theta = \pi/6$ <sup>1</sup> to obtain the optimal  $\omega$  as

$$\omega_{\text{opt}} = \frac{\sqrt{3}RC + \sqrt{3(RC)^2 + 4LC}}{2LC}.$$

If we plug all reference values into  $\omega_{\text{opt}}$ , we calculate that  $\omega_{\text{opt}} = 1.42761$  Hz.

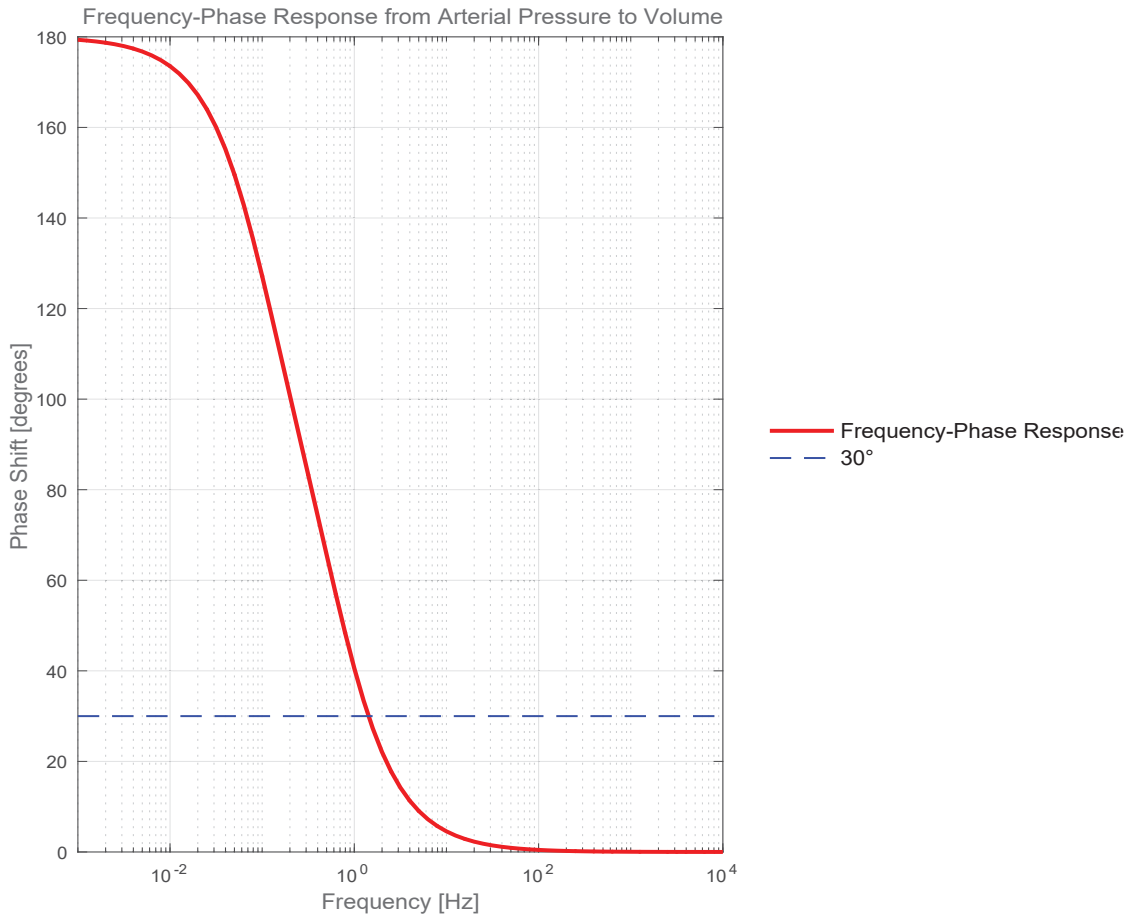


FIGURE 6. [Color online] The logarithmic plot of (19) representing the frequency–phase response from arterial pressure to volume. One can observe that below  $30^\circ$ , the frequencies quickly become very high. This indicates that it would be difficult to measure if autoregulation was taking place or not because there is virtually no time delay to tell between an active and inactive regulating response.

From Figure 6, we observe that the lower the frequency is, the easier it is to tell if an organ is autoregulating or the more out–of–phase the active regulating response is from the inactive regulating response. This can be explained by keeping in mind that Figure 5 showed an inactive regulating response is  $180^\circ$  out–of–phase with the active regulating response. Thus, the phase shift will be harder to observe the further away from  $180^\circ$  the frequency is. Higher frequencies cause shorter time delays. However, an experiment conducted at low frequencies will cause longer time delays and would take up too much time and so a “middle–ground” must be found. At a phase shift of  $30^\circ$ , the optimal frequency  $\omega_{\text{opt}}$  is obtained. In this way, an experiment

<sup>1</sup>This is a measurement consideration because it is hard to measure the phase of real signals with accuracy below  $\pi/6$ , refer to [3].

would not take too long and the time delay would be sufficient for a medical professional to be able to tell whether autoregulation was taking place or not [3].

### 3. DISCUSSION AND CONCLUSION

To conclude, in this study we successfully utilized our mathematical model for blood flow autoregulation and knowledge of mathematics to find the wall-compliance profile of the blood vessels and the frequency response of the autoregulation system. By finding the constants  $\gamma$  and  $\pi_o$ , we were able to successfully find the complete realistic wall-compliance profile. Utilizing the wall-compliance profile (4) enabled us to then find the frequency response of the autoregulation system using equations (1)–(3) and the optimal frequency. The frequency response of the autoregulation system that we determined provides doctors with a mathematical tool that can be utilized quickly and accurately to determine if autoregulation is taking place in a patient by observing the phase shift given some input frequency. We speculate that utilizing the frequency response could indicate the amount of time it takes for constant flow of blood to return to the circulatory system and therefore, to vital organs. We acknowledge that we are not qualified to explain exactly how this information would be applied for an experiment and what the details of an experiment conducted by qualified doctors and or researchers would entail. We refer readers especially to [1], [3], and [9] for information on potential experimentation and data collection with this type of mathematical analysis. In the future, we think our model and results can be compared with information and data gathered from a designed experiment by medical professionals to verify the accuracy of our model and ultimately help treat patients efficiently and effectively.

### ACKNOWLEDGEMENTS

We cannot express enough thanks to our mentor, Dr. Sebastian Acosta from Texas Children’s Hospital as well as Dr. Hyejin Kim, Dr. Yulia Hristova, and Dr. Mahesh Agarwal, our professors from University of Michigan–Dearborn during the Winter 2016 semester. We especially want to thank Dr. Hyejin Kim for her persistent support beyond the semester in guiding us through many iterations of editing this paper. We would also like to thank the 2016 PIC Math program reviewers from the Mathematical Association of America and the reviewers from SIAM Undergraduate Research Online Journal for their review and criticism.

### REFERENCES

- [1] Sebastian Acosta, Daniel J. Penny, and Craig G. Rusin, An effective model of blood flow in capillary beds, *Microvasc. Res.*, 100:40–47, 2015.
- [2] Boron, Walter, and Emile Boulpaep. *Medical Physiology. 2nd ed.*, Saunders, 2012, pp. 554-76.
- [3] Charles D Fraser, Ken M Brady, Christopher J Rhee, R Blain Easley, Kathleen Kibler, Peter Smielewski, Marek Czosnyka, David W Kaczka, Dean B. Andropoulos, and Craig Rusin, The frequency response of cerebral autoregulation, *J. Appl. Physiol.*, 115 (May 2013): 52–6, 2013.
- [4] A. Murray Harper, Autoregulation of cerebral blood flow: influence of the arterial blood pressure on the blood flow through the cerebral cortex, *J. Neurol. Neurosurg. Psychiat.*, 1966, 29, 398–403.
- [5] Mette S. Olufsen, Ali Nadim, On Deriving Lumped Models For Blood Flow and Pressure in the Systemic Arteries, *Mathematical Biosciences and Engineering*, vol. 1, no. 1, June 2004, 61–80.
- [6] R. C. Hibbler *Engineering Mechanics Dynamics 14th ed.*, Hoboken: Pearson Education, Inc., 2016.
- [7] William J. Palm. *System Dynamics*, Boston: McGraw–Hill Higher Education, 2005.
- [8] Nico Westerhof, Jan–Willem Lankhaar, Berend E. Westerhof, The arterial Windkessel, *Med. Biol. Eng. Comput.*, (2009) 47: 131–141.
- [9] Christian Zweifel, Celeste Dias, Peter Smielewski, and Marek Czosnyka, Continuous time–domain monitoring of cerebral autoregulation in neurocritical care, *Med. Eng. Phys.*, 36(5): 638–645, 2014.

UNIVERSITY OF MICHIGAN–DEARBORN, DEPARTMENT OF MATHEMATICS AND STATISTICS, DEARBORN, MI 48128  
E-mail address: nbratto@umich.edu

UNIVERSITY OF MICHIGAN–DEARBORN, DEPARTMENT OF MATHEMATICS AND STATISTICS, DEARBORN, MI 48128  
E-mail address: ahanek@umich.edu

UNIVERSITY OF MICHIGAN–DEARBORN, DEPARTMENT OF MATHEMATICS AND STATISTICS, DEARBORN, MI, 48128  
E-mail address: dwendl@umich.edu

TEXAS CHILDREN’S HOSPITAL, BAYLOR COLLEGE OF MEDICINE, DEPARTMENT OF PEDIATRICS–CARDIOLOGY, HOUSTON, TX  
E-mail address: Sebastian.Acosta@bcm.edu